15

Investigation of the real shape changes of round thin-film membranes during the bulge testing

© A.A. Dedkova, N.A. Djuzhev

National Research University of Electronic Technology,
124498 Zelenograd, Moscow, Russia
e-mail: dedkova@ckp-miet.ru

Received April 7, 2022
Revised April 7, 2022
Accepted April 7, 2022

We discuss the study of the sphericity of the real shape of round thin-film membranes when it changes during the bulge testing. Membrane structures: $SiN_x/SiO_2/SiN_x/SiO_2$, $pSi^*/SiN_x/SiO_2$, Al, etc. We described the technique for determining the areas of deviation of the membrane surface shape from a spherical one, estimating the magnitude and peculiarities of the distribution of the radius of curvature along the membrane diameter. It is shown that the shape of the membranes differs from spherical closer to the edge (perimeter), and in many cases also to the area of the top (center) of the membrane. A trend was found: an increase in the radius of curvature as it approaches the center of the membrane.

Keywords: thin films, membrane, mechanical characteristics, mechanical stresses, deformation, deflection, strain, microelectromechanical systems, MEMS, circular membrane, silicon substrate, optical profilometry, overpressure, bulge testing, bulging method, surface, topography, radius of curvature, curvature.

DOI: 10.21883/TP.2022.08.54575.86-22

Introduction

Currently the special attention is given to the issues of analysis of a stress-strain state, appearing in microelectromechanical systems (MEMS). Circular membranes fixed on the contour in terms of the membrane formed from thin films created on a silicon substrate after deep through etching of silicon from the back of the wafer (Bosch process) were studied [1–4]. Such membranes are used in X-ray optics [2], as sensitive elements of sensors of various physical quantities [5,6] and others.

To determine the mechanical characteristics of membranes (their constituent films), the bulge testing is widely used, and to analyze the experimental data obtained — relations of the theory of thin wafers and shells, with various modifications [1,2,7–22]. The method consists in applying unilateral overpressure to the membrane from its reverse side, analyzing the dependence of the deflection of the membrane on the value of the applied pressure, calculating mechanical characteristics from this dependence (Young's modulus or etc.).

At the same time, it is often assumed that the membrane under load takes a spherical shape. Earlier, the authors showed [1] that the real initial shape of the membranes formed by the Bosch process is not flat or spherical — membranes are often similar to a truncated cone, can be convex and concave, contain folds, etc. This effect is probably a consequence of residual stresses in the film on the substrate prior to the formation of the membrane. Under the influence of excessive pressure, the membrane visually becomes like a segment of a sphere — a dome convex upwards [1]. To analyze the stress-strain state of such membranes under the action of applied overpressure (P) — it is necessary to investigate in detail the change in the real shape of the membranes and assess the degree of its proximity to the sphere.

This paper is devoted to the development and use of a technique for assessing the degree of sphericity of the real shape of round thin-film membranes when it changes during the implementation of the bulge testing.

1. Equipment

The bulge testing is implemented on an apparatus developed by the authors, described in detail in previous studies. The apparatus is made on the basis of the Veeco Wyko NT 9300 optical profilometer and special equipment for fixing the test sample and applying excess pressure to it [22]. The apparatus allows you to analyze the change in the surface topography of the area with the membrane as the applied overpressure increases. The size of the measurement area is usually about $1.9-2.4$ mm, the size of the formed height matrix is 640×480 (Fig. $1, a$).

the radius of curvature R from the surface profiles (the profiles are shown in Fig. $1, b$). To do this, the operator sets the boundaries of the segment on the profile (the position of the cursors); one value of the radius of curvature for this segment is calculated. However, this software does not allow us to determine the distribution of the radius of curvature R over the profiles of the surface — depending on the change in the radius of curvature R along the profile. Also, Vision does not allow you to directly compare the

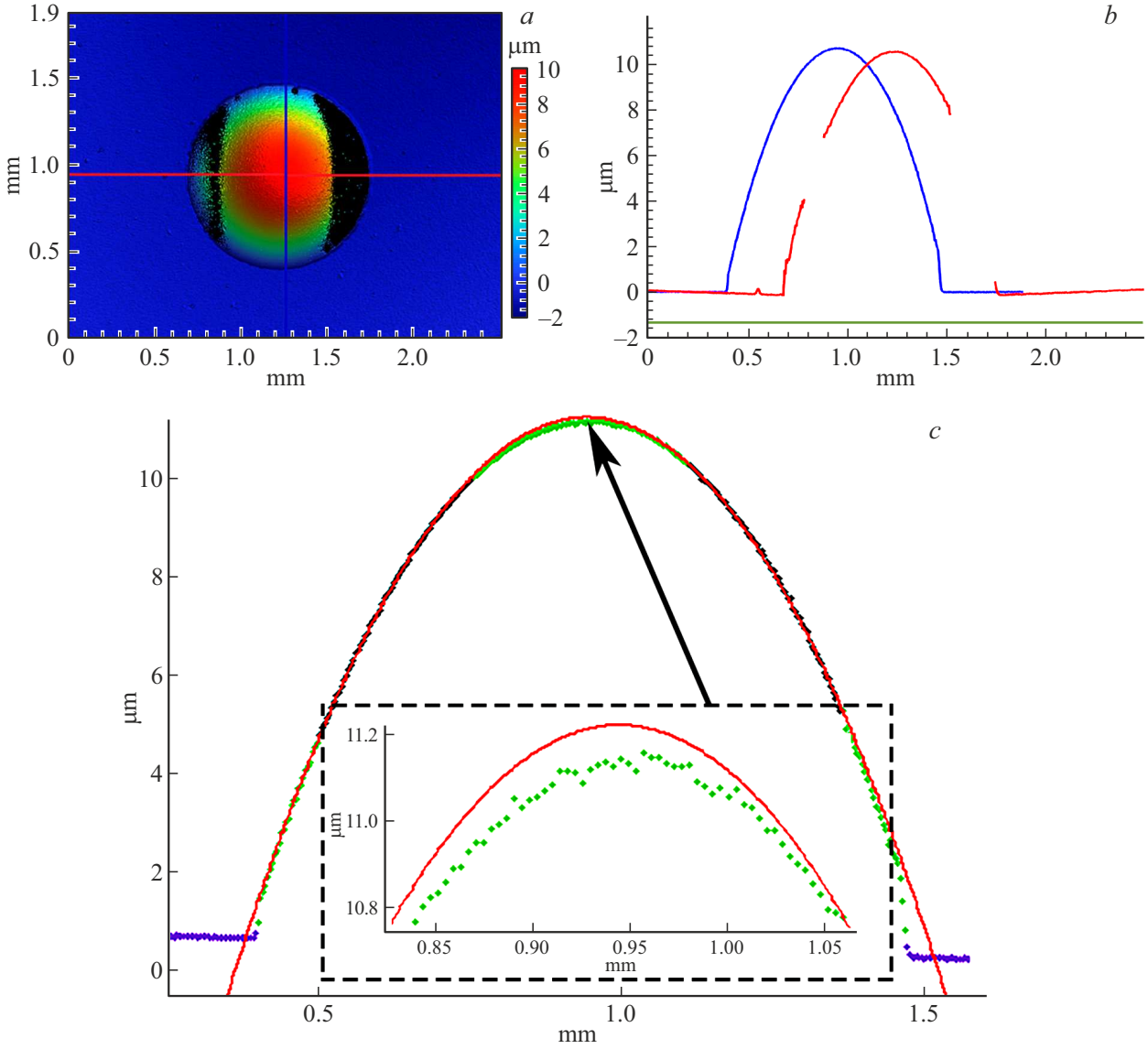

Figure 1. Topography of the area with the membrane (a) and surface profiles (b, c) of the membrane Al ($0.6\,\mu$m) at $P = 1.2$ atm. Membrane profile Al ($0.6\,\mu$m) at $P = 1.2$ atm (c): the membrane area is shown in green (light points) (color in the online version), the area used for approximation is shown in black (the darkest points), the approximation curve is shown in red (color in the online version) (smooth line), the substrate is shown in purple (color in the online version). On surface topography maps (a) here and further the color scale is from blue (lowest values) to red (highest values (color in the online version)).

approximation curves and the real surface profile (you get only information about the value of R for the selected segment — one number is output). All this peculiarities required the development of the procedure described in this paper.

2. Samples and model data

The calculation of the radius of curvature was carried out for the following data:

— experimentally obtained data for a membrane made of an Al monolayer with a thickness of $0.6\,\mu$m (Fig. 1);

— experimental data obtained for a membrane with the structure $SiN_x/SiO_2/SiN_x/SiO_2$, layer thicknesses SiN_x — $0.13\,\mu$m, SiO_2 — $0.5\,\mu$m (Fig. 2);

— experimental data obtained for multilayer Al membrane: 20 layers of Al with a total thickness of $0.6\,\mu$m, using ion bombardment after deposition of each layer (Fig. 3);

— experimental data obtained for a membrane with the structure $pSi^*/SiN_x/SiO_2$, thickness of pSi^* layers — $0.6\,\mu$m, SiN_x — $0.13\,\mu$m, SiO_2 — $0.5\,\mu$m (Fig. 4);

— experimentally obtained data for the Si membrane (Fig. 5);

— model data of a membrane formed in COMSOL Multiphysics;

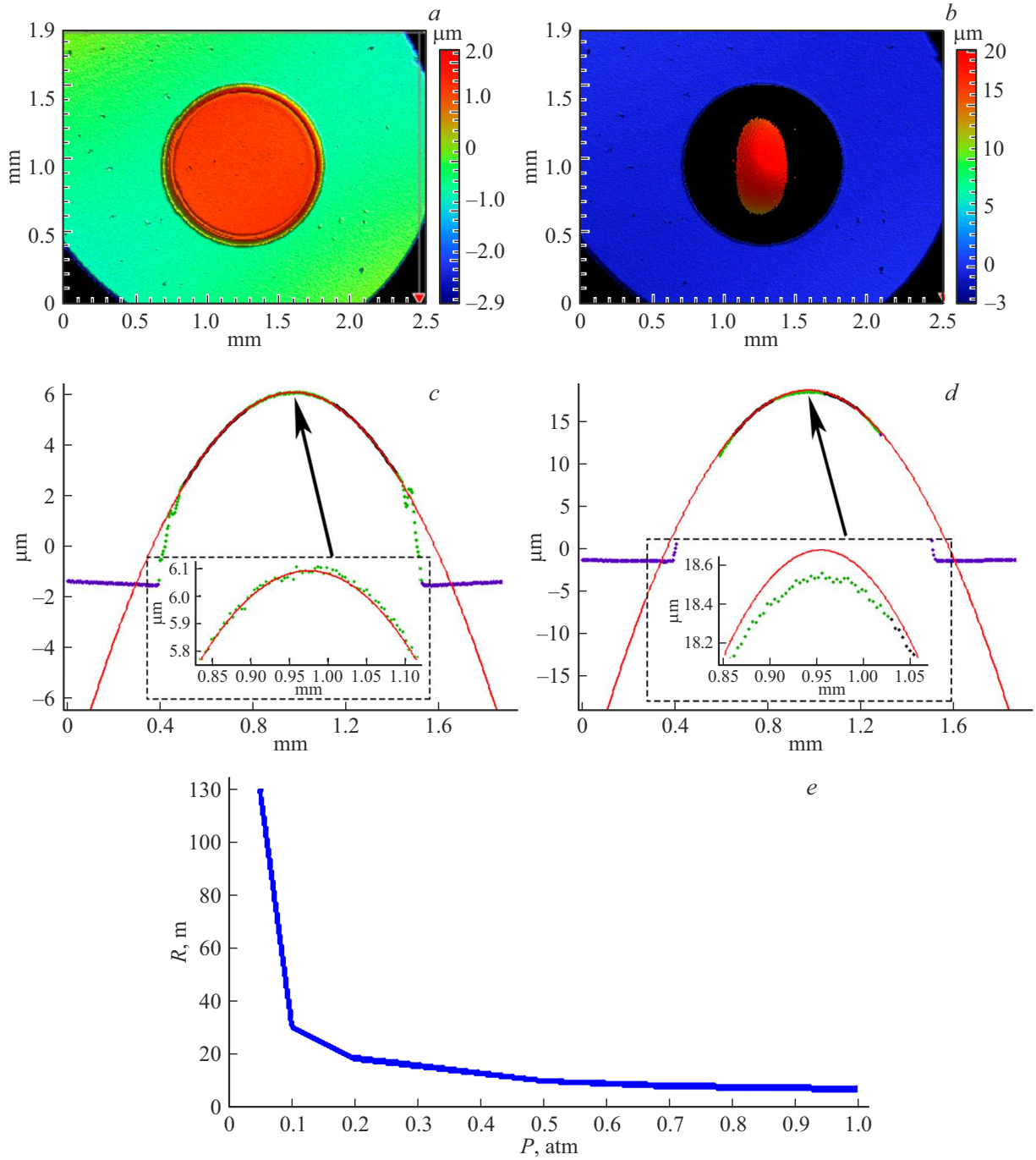

Figure 2. Topography of an area with $SiN_x/SiO_2/SiN_x/SiO_2$-membrane (a, b) and surface profiles (c, d) membranes at $P = 0$ (a), 0.1 atm (c), 0.5 atm (b, d). Color accordance of (c, d) — similar to Fig. 1, c. The dependence of the calculated radius of curvature R on the applied overpressure (e).

— model data of a noisy circular arc formed in Matlab.

The distributions of the radius of curvature are shown in Fig. 6 for the same data:

— experimentally obtained data for a membrane made of an Al monolayer with a thickness of 0.6 μm (Fig. 6);

— experimental data obtained for a membrane with the structure $SiN_x/SiO_2/SiN_x/SiO_2$, layer thickness SiN_x — 0.13 μm, SiO_2 — 0.5 μm (Figs. 6 c, d);

— model data of a membrane formed in COMSOL Multiphysics (Fig. 6, e);

— model data of a noisy circular arc formed in Matlab (Fig. 6, f).

$pSi^*/SiN_x/SiO_2$ membranes (of different diameters and thicknesses of layers), $Al/SiO_2/Al$ membranes, etc. were also analyzed, but calculated distributions for them are not presented in the present study.

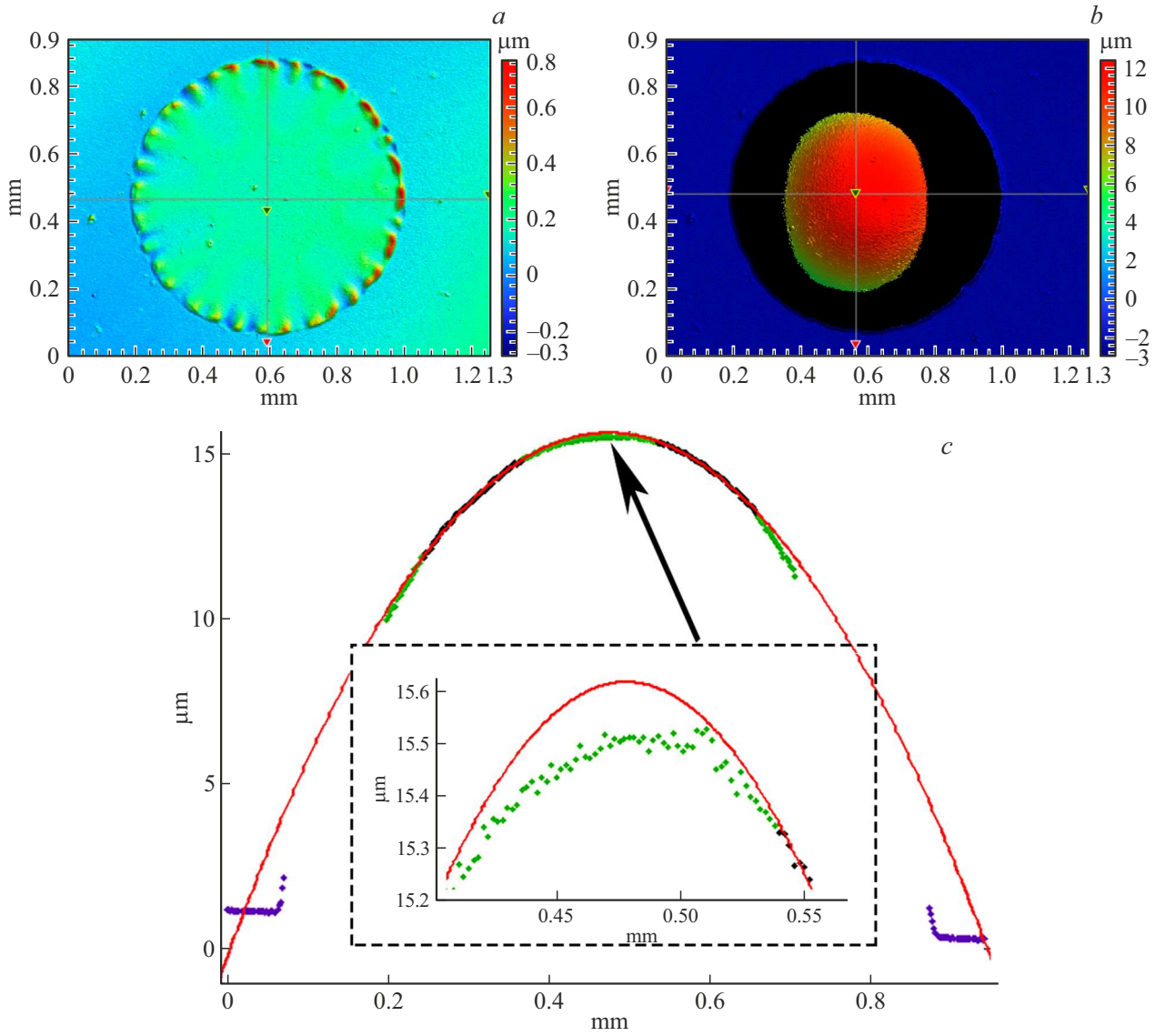

Figure 3. Topography of the region with a multilayer Al-membrane (a, b) and the surface profile (c) of the membrane at $P = 0$ (a), 1.2 atm (b, c). Color accordance of (c) — similar to Fig. 1, c.

3. Procedure

The study of the radius of curvature R by surface profiles (Fig. 2, b) was carried out in Matlab using the Curve Fitting Tool. The developed program in the Matlab environment includes:

1) reduction of initial experimental data to a form suitable for processing and analysis;

2) surface profile selection;

3) determination of the membrane location area on this profile and areas for subsequent selection of the radius of curvature (areas for approximation);

4) construction of approximation curves (representing the arcs of circles) and determination of the radius of curvature in the Curve Fitting Tool. To do this, the radius of curvature of the arc of the circle is determined as a function of $y(x)$:

$$y(x) = \sqrt{((a_1^2 - (x - b_1)^2)} + d_1, \qquad (1)$$

where a_1 — the radius of the circle, b_1 and d_1 — offsets of the vertex relative to the origin.

At the first stage of the research, the correspondence between the shape of the membrane and the circle of the selected radius of curvature approximating the experimental points of the arc was evaluated. First, the part of the profile related to the membrane and the part of the profile related to the substrate were determined. On Fig. 1, c the green color (light dots) (color in the online version) shows the membrane profile, purple (color in the online version) — substrate surface profile. Then the lateral surface of the membrane was highlighted without using areas closer to the center (top) of the membrane and closer to fixing

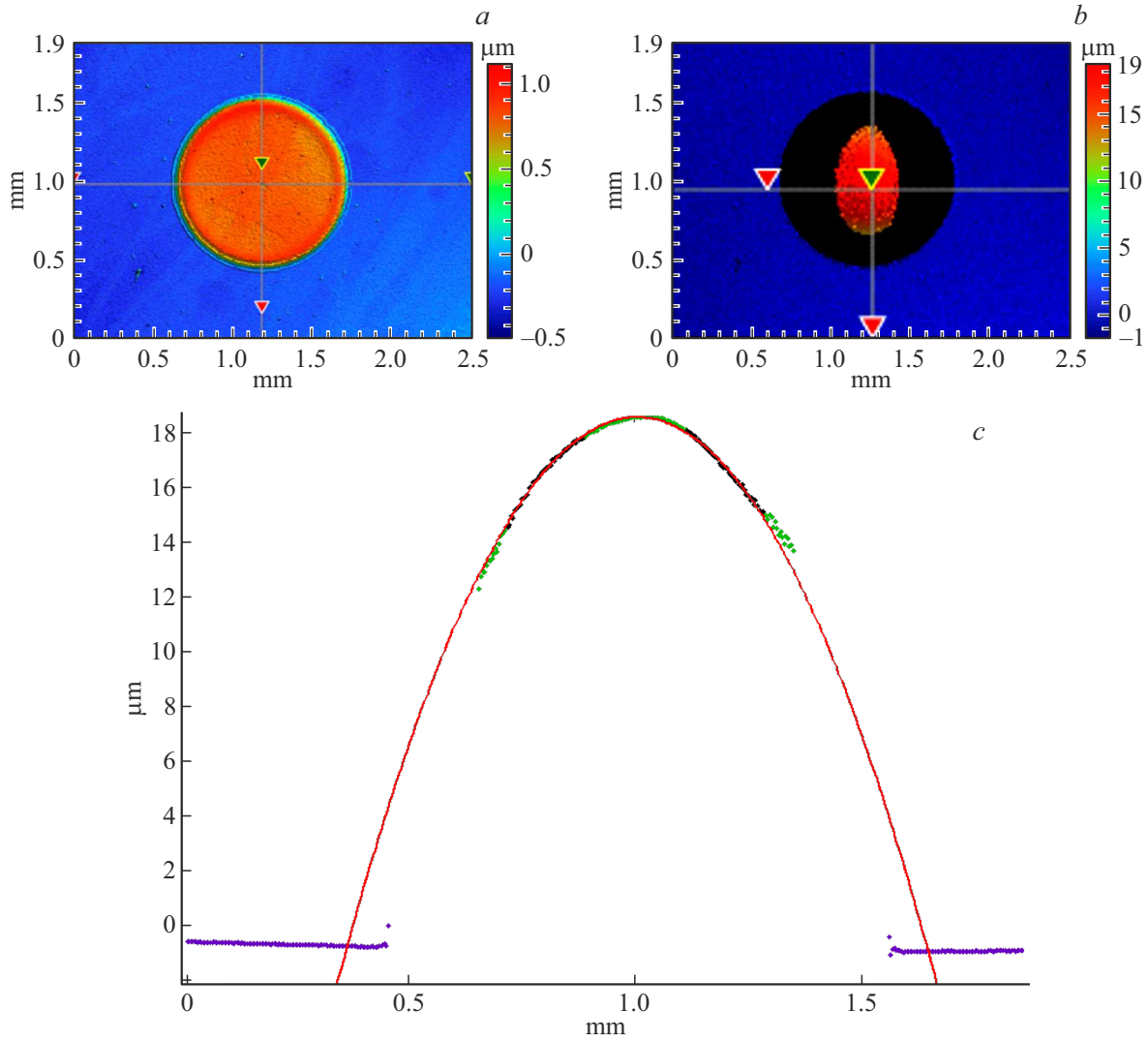

Figure 4. Topography of the region with the $pSi^*/SiN_x/SiO_2$-membrane (a, b) and the surface profile (c) of the membrane at $P = 0$ (a), 0.6 atm (b, c). Color accordance of (c) — similar to Fig. 1, *c*.

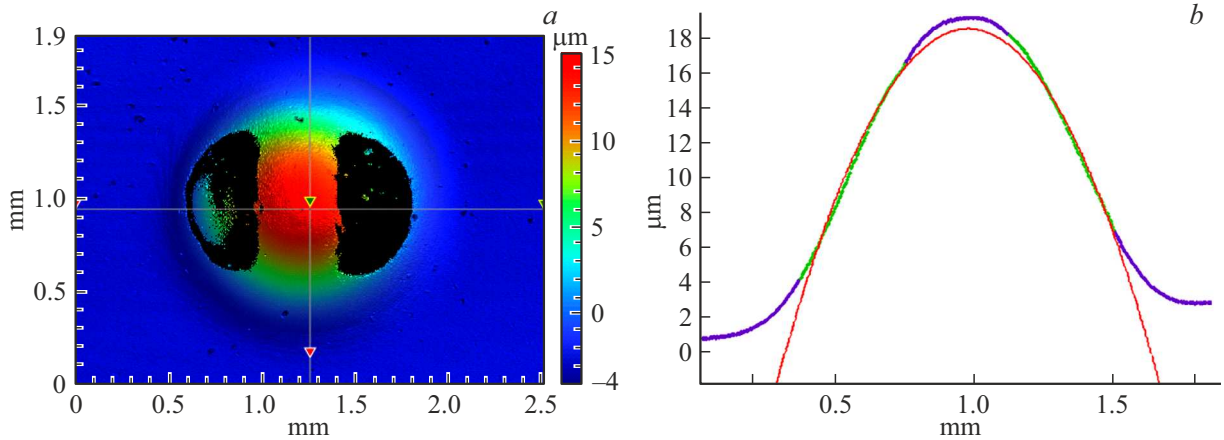

Figure 5. Topography of the area with the Si-membrane (a) and the surface profile (b) of the membrane at $P = 1.0$ atm. *b* — dark purple shows experimental data, data used for approximation area is shown in light green, approximation curve is shown in red (light smooth line) (color in the online version).

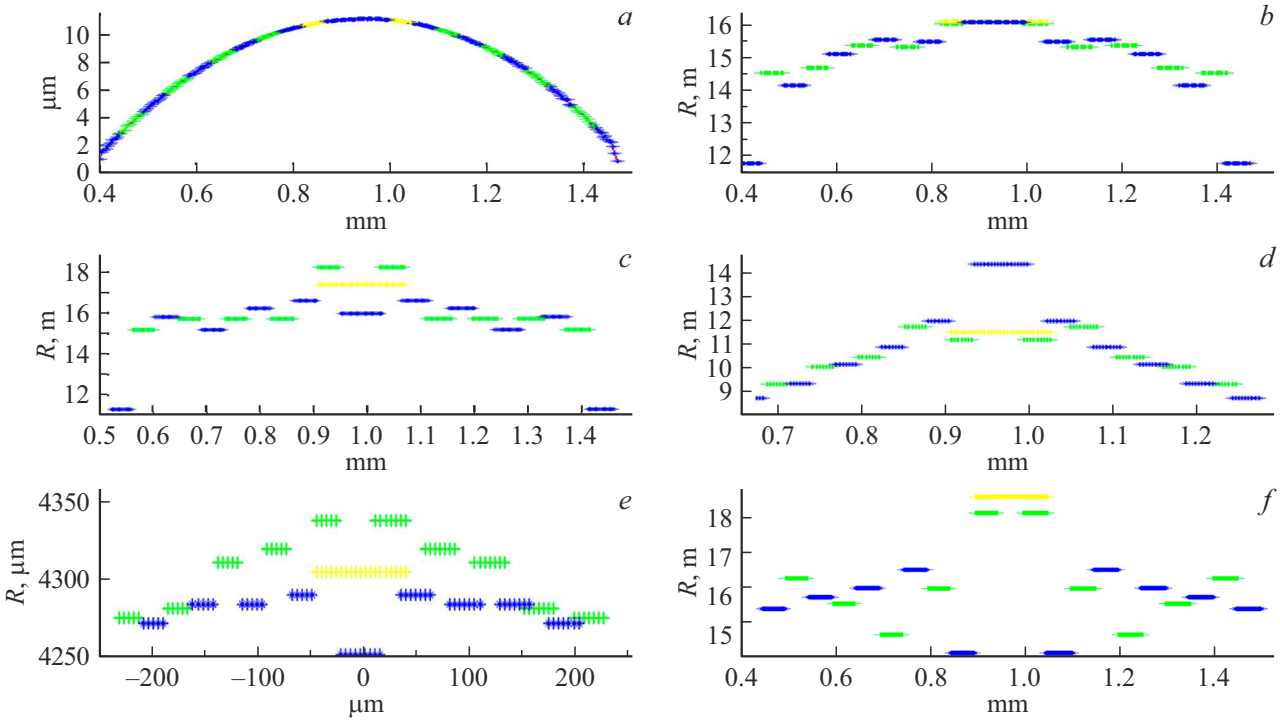

Figure 6. Membrane profile Al ($0.6\,\mu$m) at $P = 1.2$ atm divided into segments (a) and the corresponding distribution of the radius of curvature R (b); distributions R for the membrane $SiN_x/SiO_2/SiN_x/SiO_2$ at $P = 0.3$ atm (c), 0.5 atm (d); distribution R for a Comsol membrane (e); distribution R for noisy model data of a circular arc (f). For clarity, adjacent segments are shown in different colors.

(in Fig. 1, c this area is shown in black). After that, an approximation curve was selected for both cases — both over the entire surface of the membrane (the lighter green area) and over part of the lateral surface (the dark black area). Subsequently, the results of approximation along the side surface were mainly used for analysis. The radius of curvature R was determined and the discrepancy between the experimental data and the approximation curve was estimated (Fig. 1, c — the region of the membrane edge and the inset).

At the second stage of the research, the distribution of R was analyzed, for which the data on the lateral surface of the membrane were divided into several pairs of segments of the same length (Fig. 6, a), approximation curves were selected (its own circular arc for each pair of segments), the radius of curvature R was calculated for each pair. A pair of segments was used in connection with the need for data on both sides of the top of the membrane for qualitative approximation. Fig. 6, for clarity, adjacent segments shows in different colors (lighter — green and darker —blue (color in the online version)). At the same time, in the area of the top of the membrane, due to the limitations of the calculation technique, data on a segment including three central segments are also given. An approximation was also carried out for this combined segment; the corresponding value of the calculated radius of curvature is shown in the lightest (yellow (color in the online version)). That is, in the area of the top of the membrane, it is worth focusing on this value (yellow) of the calculated radius of curvature R.

4. Calculation results based on experimental data

Fig. 1, c shows: a selected approximation curve with a radius of curvature of 14.96 m and an experimental profile for the membrane Al ($0.6\,\mu$m) at $P = 1.2$ atm. It can be seen that these curves do not perfectly match each other: there is a discrepancy in the area of the membrane attachment (closer to the substrate), as well as in the area closer to the center of the membrane (the enlarged image is shown in the inset in Fig. 1, c). Fig. 6, b shows the corresponding distribution of the radius of curvature R for this membrane. It can be seen that the radius of curvature R tends to increase as it approaches the center (vertex) of the membrane.

The study of changes in the radius of curvature of $SiN_x/SiO_2/SiN_x/SiO_2$ membranes was carried out on a series of formed experimental data: in the range of changes in the applied pressure from 0.05 to 1.0 atm. Fig. 2, c, d shows the approximation curve and experimental profile at $P = 0.1$ atm. (Fig. 2, c, radius of curvature 30.3 m) and $P = 0.5$ atm (Fig. 2, d, radius of curvature 9.9 m). One can see the divergence of these curves in the area closer to the membrane fixation in both cases, and at a higher pressure — and in the area closer to the center of the

membrane (the situation persists in case of increasing pressure). Fig. 2, *e* shows the dependence of the radius of curvature R as the applied overpressure increases. As expected, the radius of curvature R is gradually decreasing. Fig. 6, *c, d* shows the distributions of the radius of curvature R at pressures $P = 0.3$ (Fig. 6, *c*), and 0.5 atm (Fig. 6, *d*); there is a tendency to increase the radius of curvature as it approaches the center of the membrane.

Fig. 3, *c* shows data for a multilayer Al membrane at $P = 1.2$ atm, the calculated radius of curvature R was 7.1 m. There is also a significant discrepancy in the area of membrane fixation and a slight discrepancy closer to the center of the membrane.

Fig. 4, *c* shows data for $pSi^*/Si_3N_4/SiO_2$ membranes at $P = 0.6$ atm, the calculated radius of curvature R was 10.6 m. There is a significant discrepancy in the area of membrane fixation, the curves coincide closer to the center of the membrane.

Fig. 5, *b* shows data for a multiplayer Al membrane at $P = 1.0$ atm, the calculated radius of curvature R was 11.8 m. It can be seen that the shape of the profile is significantly influenced by the fact of the composition of this membrane exclusively from Si (there is no sharp transition in the fixing area, which is presumably caused by the peculiarities of the fastening, underpickling, etc.). This data is given mainly for comparison with the features of other membranes.

The radius of curvature determined by the surface profiles in Vision software correspond to those calculated according to the described technique, which indicates the correctness of its operation.

The described results are given for the case of approximation along the lateral surface of the membrane (dark black area; exception — Si-membrane analysis, where the lateral surface was also used, but in Fig. 5, *b* it is shown in light green (color in the online version)). However, it should be taken into account that these discrepancies (both in the area of fixation and closer to the center of the membrane) were also present in the case of approximation over the green area (containing the entire membrane, including its vertex).

Separately, it should be noted that in some cases, when analyzing membrane profiles, especially if there is a significant amount of initial deflection (about 10 μm or more) and/or folds on the membranes — directly by the shape of the membrane under pressure or by the profiles of the membrane, it was possible to visually observe a flatter an area or area with small folds in the center of the membrane. This effect was observed on membranes with such a structure as $Al/SiO_2/Al$, $Be/SiO_2/Si$, some Al-membranes manufactured in various ways, etc.

5. Calculation results based on model data

When performing calculations based on the data obtained in Comsol, an almost perfect correspondence between the shape of the model data and the calculated approximation curve was observed (only the center of the membrane was analyzed), the radius of curvature 4266 μm. When analyzing the dependence of the change in the radius of curvature R, a weak tendency to increase R as it approaches the center of the membrane was also observed (Fig. 6, *e*).

Since it was found for all the analyzed membranes that the radius of curvature tends to increase as it approaches the top of the membrane, calculations based on the model distribution of the circular arc were given to assess the correctness of the calculation technique. To do this, in accordance with the expression (1), a data set was formed corresponding to the studied membranes in terms of the ratio of the radius of curvature and the height of the analyzed segment, as well as in order of the radius of curvature: $a_1 = 15.692\,\mu$m (radius of the circle for the profile).

When calculating on an ideal data set (strictly according to the expression (1)) for all segments of the partition, the radius of curvature was 15.69 μm (corresponded to the specified one).

Then, for a better approximation of the model distribution to the real experimental data, noise, linear slope, and a change in the vertex position were additionally superimposed on the model distribution. In this case, when calculating the distribution of the radius of curvature, Fig. 6, *f* was obtained. Based on this figure, it can be concluded that there is no obvious increase or decrease in the radius of curvature as we approach the vertex according to this data. Exception — calculation at the very top, which may be a consequence of limitations of the calculation technique. However, since the effect of increasing the radius of curvature was previously observed not only in close proximity to the center of the membrane, it is likely that it is still a fact, and not a consequence of the limitations of the technique.

6. Summary

When examining the membranes the following was found:

— On all experimentally obtained data on membranes, there is a discrepancy closer to the region of membrane fixation (along its perimeter, at the boundary with the substrate), i.e. the features of the stress-strain state in this region should be analyzed, taking into account this mismatch of shape. The specific numerical value of the discrepancy can be estimated from the above images.

— A different effect is observed on different membranes: in some cases, in the area of its apex, the membrane has a slightly different radius of curvature from the main part of the membrane R (it is flatter), in others — no (the curves perfectly match). In the vast majority of cases, this flatter area is present; it can also be observed directly on the surface profile itself in the Vision software (in the area of

the top of the membrane), including as a section with small folds.

— When analyzing the distributions of the radius of curvature R, it was found that R tends to increase as it approaches the center of the membrane (vertex). Such a trend was not detected on the test array of the arc of the data circle.

— Based on the data obtained, it can be concluded that the membrane most similar to the sphere is along its lateral surface.

Conclusion

A procedure has been developed for assessing the degree of sphericity of the real shape of round thin-film membranes formed by the Bosch process when it changes during the implementation of the bulge testing based on the study of membrane surface profiles. Approbation of the procedure was carried out on various membranes: $SiN_x/SiO_2/SiN_x/SiO_2$, $pSi^*/SiN_x/SiO_2$, Al, etc.

On all the analyzed membranes, it was found that the shape of the membrane differs most from the spherical one closer to the region of attachment, on many membranes — also in the region of the apex (center) of the membrane (Figs. 1, *c*; 2, *d*; 3, *c*). There is also a tendency to increase the radius of curvature as it approaches the center of the membrane.

Funding

The work was performed using the equipment of the R&D Center of the „MEMSEC“ (MIET) with the financial support of the Ministry of Education and Science of Russia (№ 075-03-2020-216, 0719-2020-0017, mnemocode FSMR-2020-0017).

Conflict of interest

The authors declare that they have no conflict of interest.

References

[1] A.A. Dedkova, P.Yu. Glagolev, E.E. Gusev, N.A. Dyuzhev, V.Yu. Kireev, S.A. Lychev, D.A. Tovarnov. ZhFT, **91** (10), 1454 (2021). (in Russian) DOI: 10.21883/0000000000
[2] N.A. Djuzhev, E.E. Gusev, A.A. Dedkova, D.A. Tovarnov, M.A. Makhiboroda. Tech. Phys., **65** (11), 1755 (2020). DOI: 10.1134/S1063784220110055
[3] A.A. Dedkova, N.A. Dyuzhev, E.E. Gusev, M.Yu. Shtern. Rus. J. Nondestructive Testing, **56** (5), 452 (2020). DOI: 10.1134/S1061830920050046
[4] V.Yu. Kireev. *Nanotekhnologii v mikroelektronike. Nanolitografiya — protsessy i oborudovanie* (Izdatelskiy dom „Intellekt“, Dolgoprudny, 2016) (in Russian)
[5] A. Nazarov, I. Abdulhalim. Sensors and Actuators A: Phys., **257**, 113 (2017). DOI: 10.1016/j.sna.2017.02.020
[6] C. Zorman. *Material Aspects of Micro- and Nanoelectromechanical Systems* (Springer Handbook of Nanotechnology, Springer-Verlag, Berlin 2007)
[7] F. Zhao. Proceedings Modeling, Signal Processing, and Control for Smart Structures, **6926**, 69260W (2008). DOI: 10.1117/12.775511
[8] R.H. Plaut. Acta Mech., **202**, 79 (2009). DOI: 10.1007/s00707-008-0037-3
[9] J. Neggers, J.P.M. Hoenagels, F. Hild, S. Roux, M.G.D. Geers. Experimental Mechanics, **54** (5), 717 (2014). DOI: 10.1007/S11340-013-9832-4
[10] L.E. Andreeva. *Uprugie elementy priborov* (Mashgiz, M., 1962) (in Russian)
[11] S.P. Timoshenko, S. Voynovsky-Kriger. *Plastinki i obolochki* (Nauka, M., 1966) (in Russian).
[12] G. Machado, D. Favier, G. Chagnon. Experimental Mechanics, **52**, 865 (2012). DOI: 10.1007/s11340-011-9571-3
[13] A. Degen, J. Voigt, B. Sossna, F. Shi, I.W. Rangelow. Proceedings SPIE, **3996**, 97 (2000).
[14] M.K. Small, W.D. Nix. J. Mater. Res., **7** (6), 1553 (1992).
[15] A.V. Korlyakov. Nano- i mikrosistemnaya tekhnika, **8**, 17 (2007) (in Russian).
[16] O.N. Astashenkova. *Fiziko-tekhnologicheskie osnovy upravleniya mekhanicheskimi napryazheniyami v tonkoplenochnykh kompozitsiyakh mikromekhaniki.*. Diss. (SPbGEU„LETI“, St. Petersburg, 2015), 143 p. (in Russian).
[17] N.M. Yakupov, S.N. Yakupov. Stroitel'naya mekhanika inzhenernykh konstruktsiy i sooruzheniy, **1**, 6 (2017) (in Russian).
[18] A.A. Sachenkov. *Tsikl lektsiy po teorii plastin i obolochek: uchebnoe posobie* (Kazanskij universitet, Kazan, 2018) (in Russian).
[19] M.S. Ganeeva, V.E. Moiseeva, Z.V. Skvortsova. Uchenye zapiski Kazanskogo universiteta. Seriya fiziko-matematicheskie nauki, **160** (4), 670 (2018) (in Russian).
[20] A.A. Dedkova, P.Yu. Glagolev, G.D. Demin, E.E. Gusev, P.A. Skvortsov. 2020 IEEE Conf. Rus. Young Researchers in Electrical and Electronic Engineering (EIConRus), 2288 (2020). DOI: 10.1109/EIConRus49466.2020.9039289
[21] S. Jianbing, L. Xiang, X. Sufang, W. Wenjia. Interna. J. Polymer Sci., **2017**, 4183686 (2017).
[22] E.E. Gusev *Issledovanie i razrabotka tekhnologii sozdaniya vysokoprochnykh membran dlya preobrazovateley fizicheskikh velichin*. Diss. (MIET, M., 2019), 182 p. (in Russian).